

Supplementary Materials

Inhibiting WNT Ligand Production for Improved Immune Recognition in the Ovarian Tumor Microenvironment

Whitney N. Goldsberry, Selene Meza-Perez, Angelina I. Londoño, Ashwini A. Katre, Bryan T. Mott, Brandon M. Roane, Nidhi Goel, Jaclyn A. Wall, Sara J. Cooper, Lyse A. Norian, Troy D. Randall, Michael J. Birrer and Rebecca C. Arend

Gene	Cell Type
BLK	B cell
CD19	B cell
FCRL2	B cell
MS4A1	B cell
KIAA0125	B cell
TNFRSF17	B cell
TCL1A	B cell
SPIB	B cell
PNOC	B cell
PTPRC	CD45 ⁺
PRF1	Cytotoxic Cells
GZMA	Cytotoxic Cells
GZMB	Cytotoxic Cells
NKG7	Cytotoxic Cells
GZMH	Cytotoxic Cells
KLRK1	Cytotoxic Cells
KLRB1	Cytotoxic Cells
KLRD1	Cytotoxic Cells
CTSW	Cytotoxic Cells
GNLY	Cytotoxic Cells
LAG3	Exhausted CD8 ⁺
CD244	Exhausted CD8 ⁺
EOMES	Exhausted CD8 ⁺
PTGER4	Exhausted CD8 ⁺
CD68	Macrophage
CD84	Macrophage
CD163	Macrophage
MS4A4A	Macrophage
FPR1	Neutrophil
SIGLEC5	Neutrophil
CSF3R	Neutrophil

FCAR	Neutrophil
FCGR3B	Neutrophil
CEACAM3	Neutrophil
S100A12	Neutrophil
KIR2DL3	NK CD56dim
KIR3DL1	NK CD56dim
KIR3DL2	NK CD56dim
IL21R	NK CD56dim
XCL1	NK cells
XCL2	NK cells
NCR1	NK cells
CD6	T cell
CD3D	T cell
CD3E	T cell
SH2D1A	T cell
TRAT1	T cell
CD3G	T cell
TBX21	Th1
CD8A	CD8 ⁺ T cell

(a)

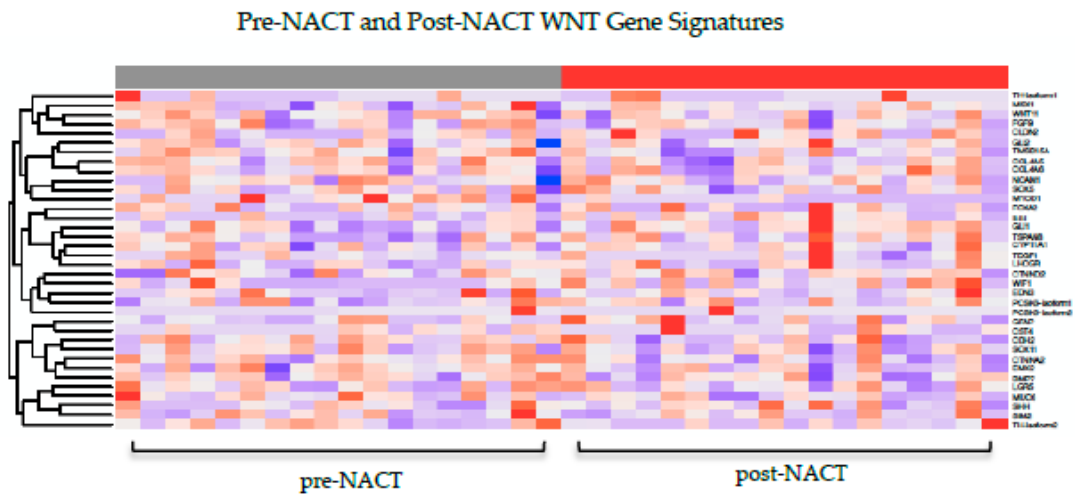
WNT Gene
TH-isoform1
MSX1
WNT11
FGF9
CLDN2
GLI2
TMSB15A
COL4A5
COL4A6
NCAM1
SOX5
MYOD1
FOXA2
IHH
GLI1
TSPAN8
CYP11A1
TDGF1

LHCGR
CTNND2
WIF1
EDN3
PCSK6-isoform1
PCSK6-isoform2
GFAP
CST4
CDH2
SOX11
CTNNA2
EMX2
BMP7
LGR5
MUC6
SHH
SIM2
TH-isoform2

(b)

RIN Values
8.4
7.8
6.0
8.5
8.9
8.1
7.5
7.2
8.3
5.8
2.4
8.4
8.1
8.4
8.7
3.1
8.3
6.2

(c)



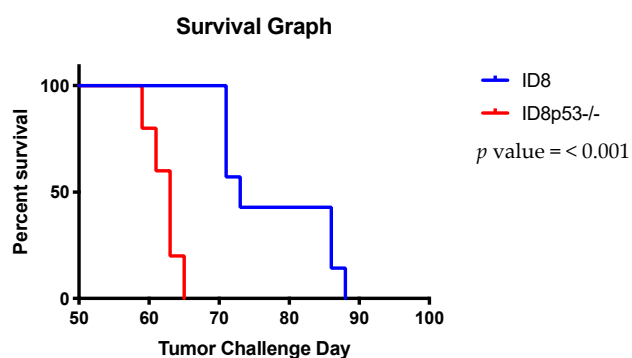
Pre-NACT Post-NACT WNT fold change PFS (months)

Pre-NACT	Post-NACT	WNT fold change	PFS (months)
Hot	Hot	0.88	33.2
Cold	Intermediate	0.85	25.7
Hot	Hot	0.96	22.7
Intermediate	Hot	1.03	19.7
Hot	Intermediate	0.95	17.6
Cold	Hot	0.99	12.6
Intermediate	Hot	1.06	10.0
Intermediate	Hot	1.04	9.5
Intermediate	Cold	1.19	9.2
Cold	Cold	1.05	8.2
Cold	Hot	0.92	6.9
Intermediate	Cold	1.04	6.8
Cold	Cold	1.01	6.4
Hot	Hot	1.00	5.1
Intermediate	Intermediate	1.05	4.2

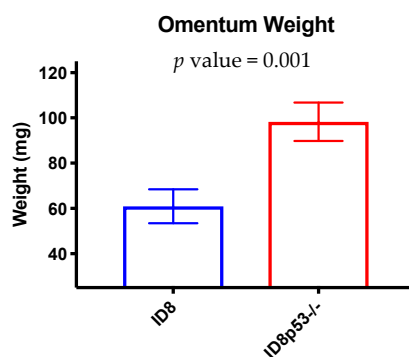
Cold	Cold	1.00	4.0
Hot	Cold	0.97	3.7

(e)

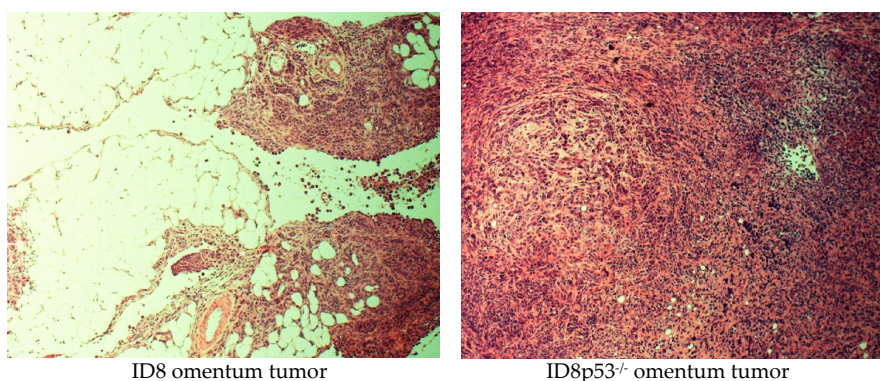
Figure S1. Wnt and immune gene signature in ovarian cancer patient samples. (a) Genes used to determine T cell signature with associated cell type. (b) Genes used to determine WNT activity. (c) RNA Integrity Numbers (RIN) for samples that were measured. (d) Heatmap with matched pre-NACT and post-NACT WNT gene signatures. (e) Matched pre-NACT and post-NACT T cell signature assignments, WNT fold change, and PFS.



(a)



(b)



(c)

Figure S2. ID8 and ID8p53^{-/-} differences of survival and tumor burden. (a) Survival was increased with ID8 intraperitoneal tumor challenge in C57Bl/6 mice compared with ID8p53^{-/-} tumor challenge. (b) On tumor challenge day 42, omentum weights between ID8 and ID8p53^{-/-} tumor challenge were statistically different. (c) Hematoxylin and eosin stained formalin fixed paraffin embedded tissue samples of omentum tumor after 42 days of tumor challenge with ID8 or ID8p53^{-/-} cells.

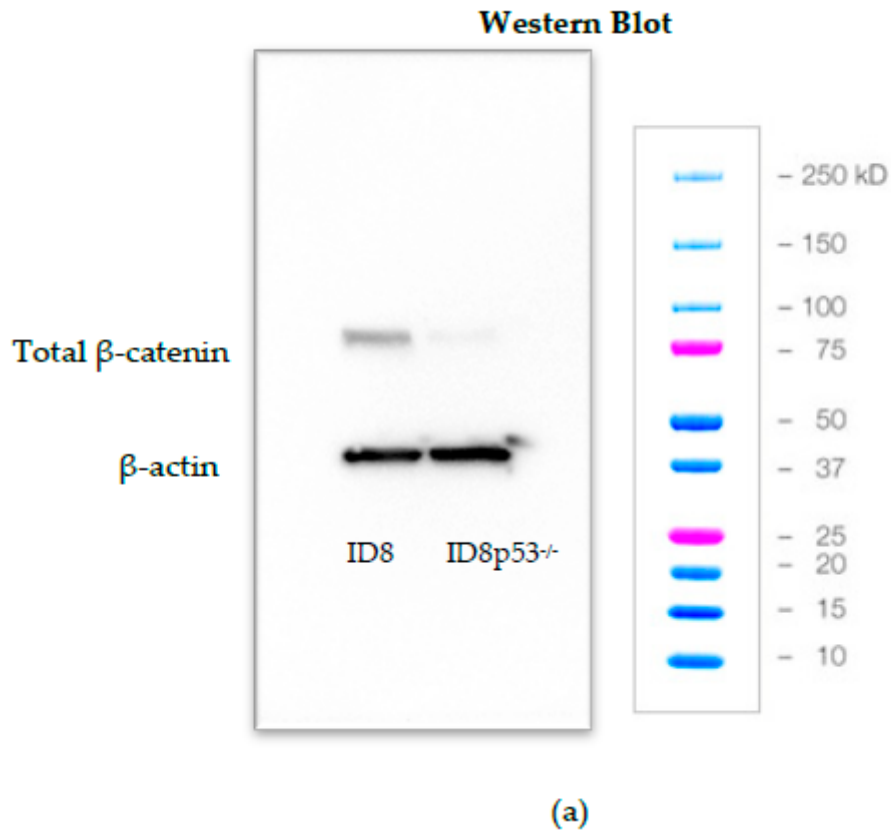
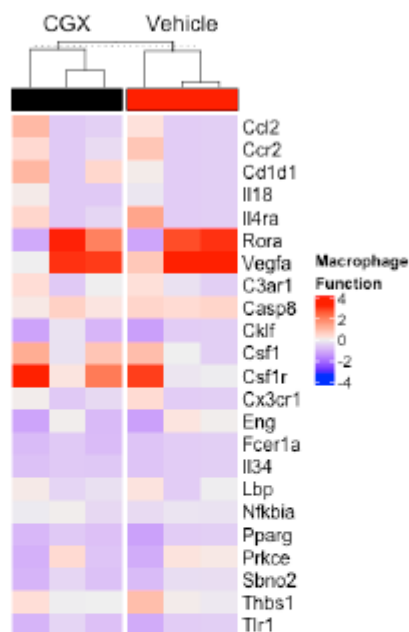
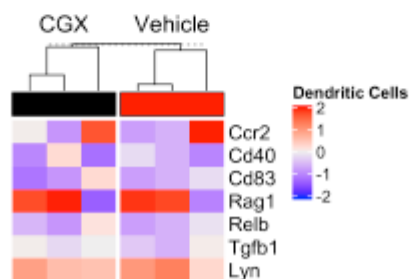


Figure S3. Comprehensive Western blot. (a) Reduced baseline β-catenin levels in the ID8p53^{-/-} cell line are evident with control β-actin levels and molecular weight ladder.

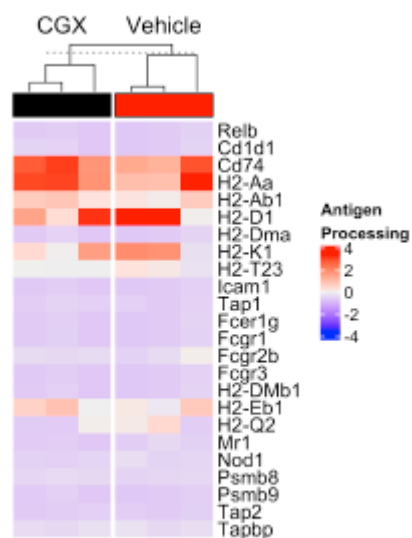
(a)



(b)

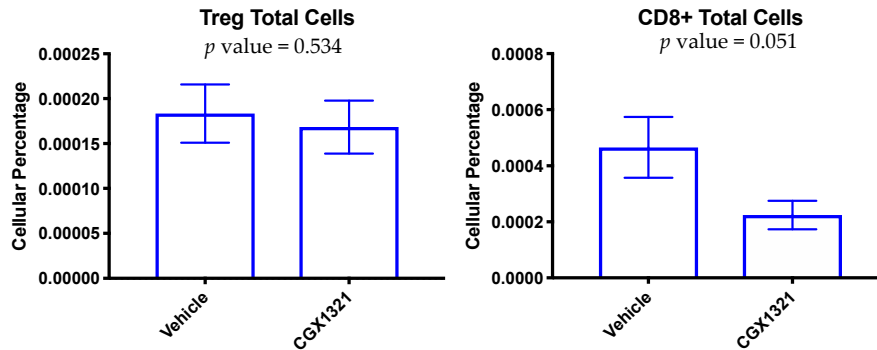


(c)



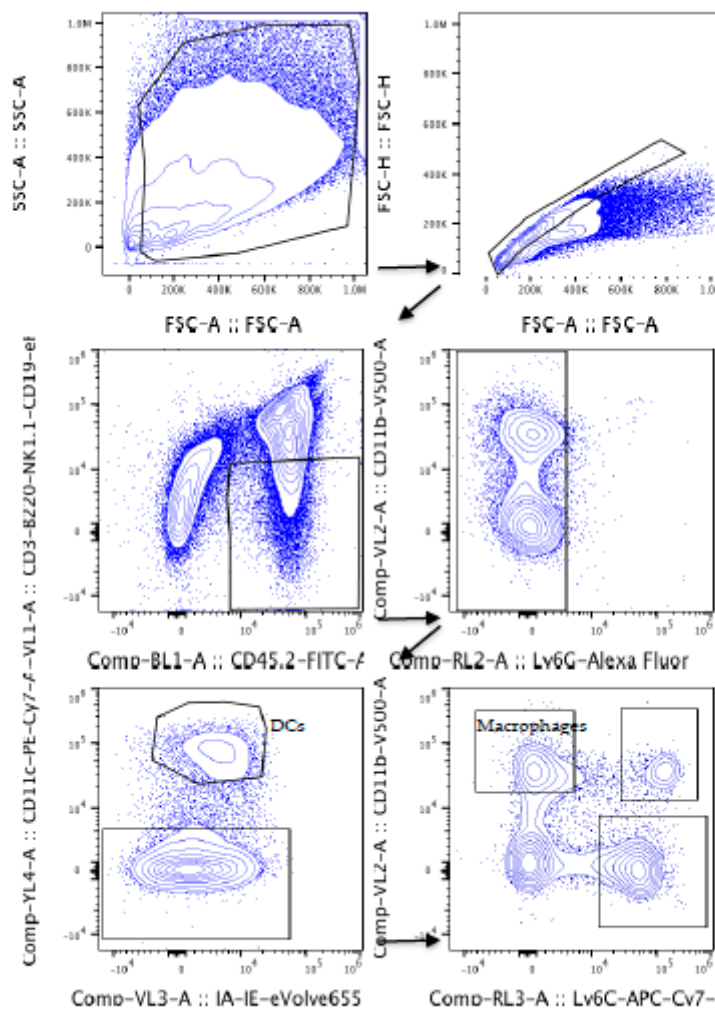
(d)

Figure S4. *In vivo* effect of Wnt signaling inhibition in omentum tumor and the microenvironment. Heatmaps, with signature gene lists, associated with each pathway signature score for NanoString analysis of omentum at 42 days tumor challenge with ID8 cells, with or without CGX1321 treatment, including gene signatures for T cell functions (a), macrophage functions (b), dendritic cell functions (c), and antigen processing (d).

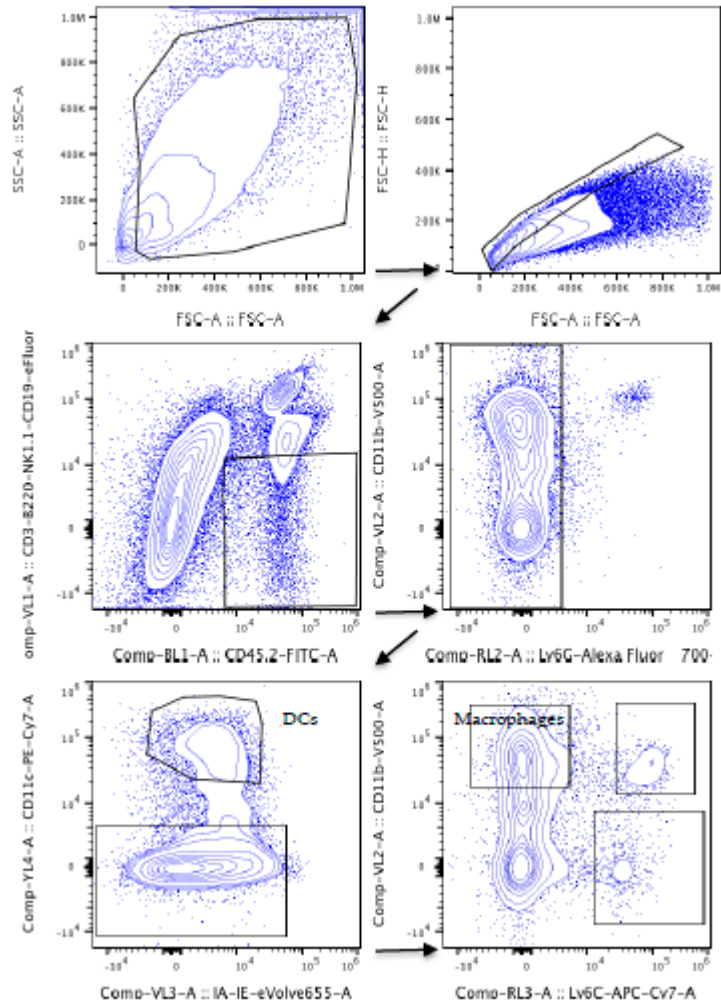


(a)

Figure S5. *In vivo* effect of Wnt signaling inhibition in omentum tumor and the microenvironment. (a) After 42 days of ID8 tumor challenge in C56Bl/6 mice, flow cytometry of omentum tumor did not reveal a statistical difference in Treg and CD8+ T cellular percentages with CGX1321 treatment.



(a)



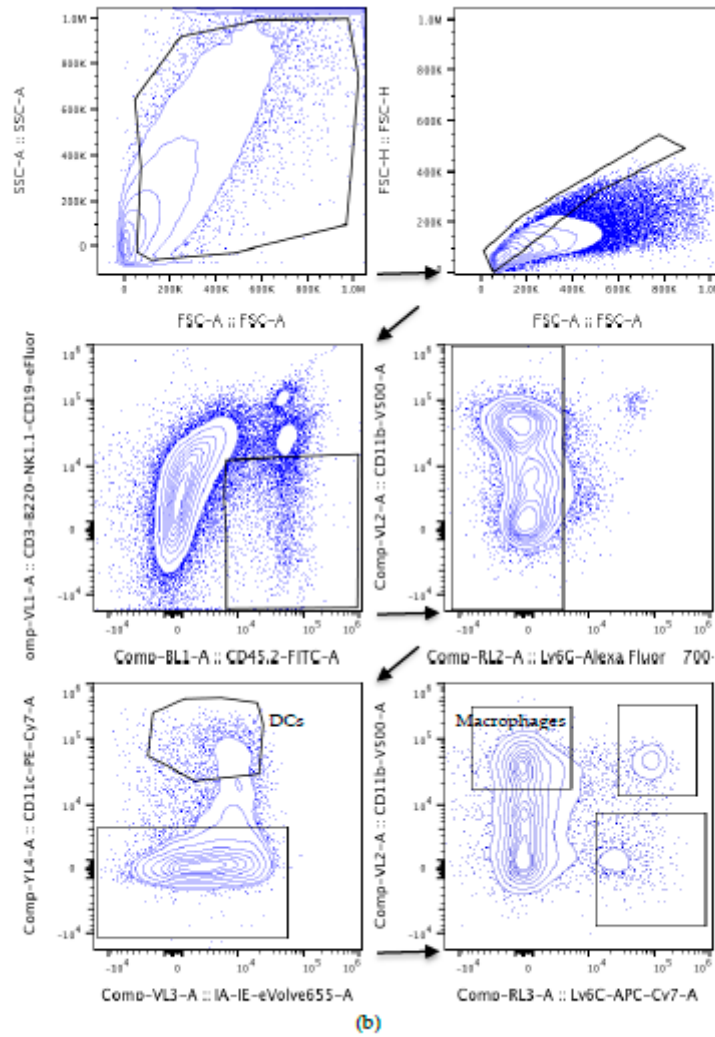
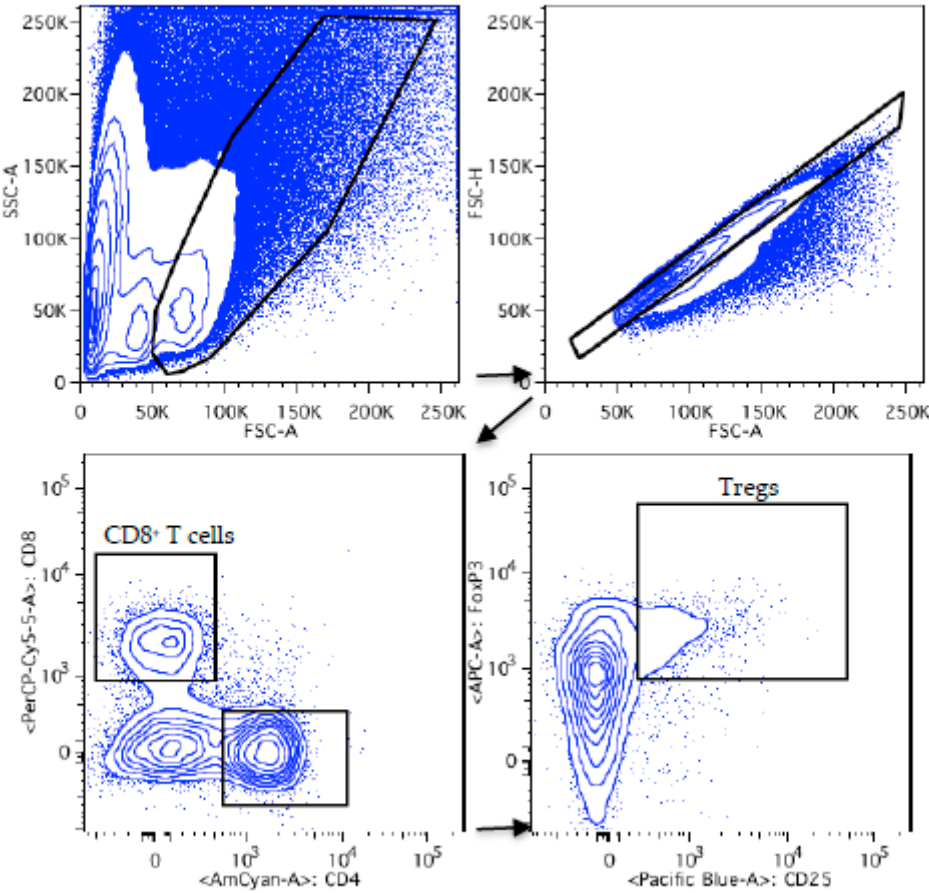
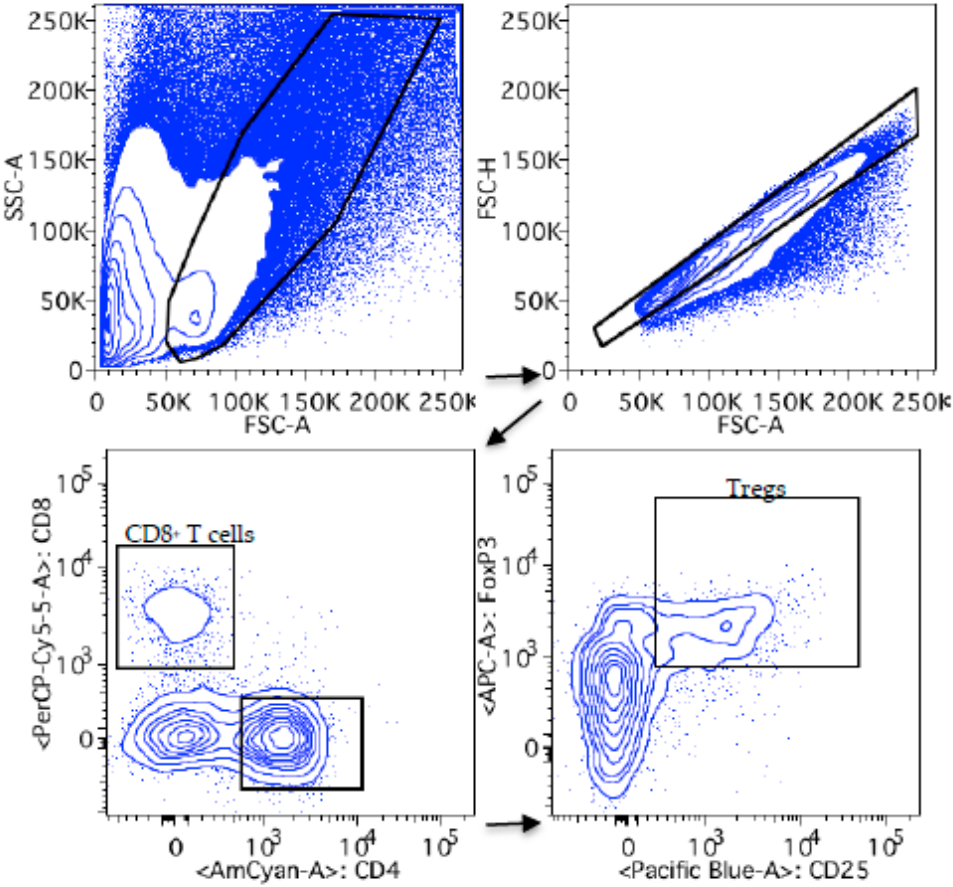


Figure S6. DC and macrophage flow cytometry gating strategy. Cell population selection narrowed from left to right, as displayed by black arrows. (a) Gating strategy for naive mouse omentum, without tumor. (b) Gating strategy for omentum tumor with mice treated with vehicle. (c) Gating strategy for omentum tumor for mice treated with CGX1321.



(a)



(b)

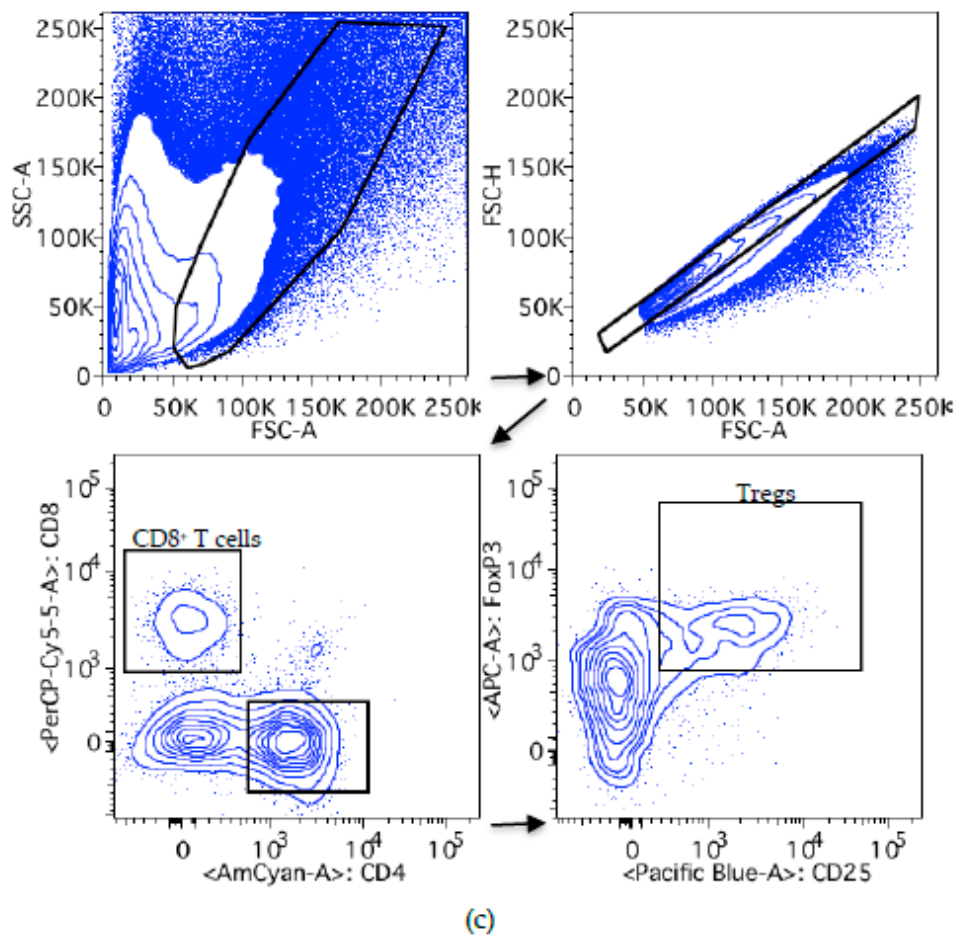
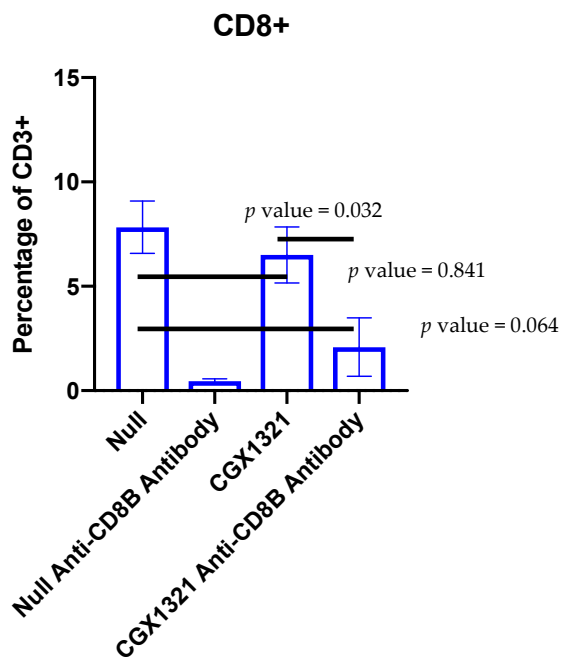


Figure S7. Treg and CD8+ T cell flow cytometry gating strategy. Cell population selection narrowed from left to right, as displayed by black arrows. (a) Gating strategy for naive mouse omentum, without tumor. (b) Gating strategy for β -catenin^{-fl/fl} mouse omentum tumor. (c) Gating strategy for CD11c-cre x β -catenin^{-fl/fl} mouse omentum tumor.



(a)

Figure S8. Anti-CD8+ β antibody with decreased CD8+ T cells. (a) Flow cytometry confirmed a decrease in CD8+ T cells in the omentum of mice treated with anti-CD8+ β antibody.



© 2020 by the authors. Licensee MDPI, Basel, Switzerland. This article is an open access article distributed under the terms and conditions of the Creative Commons Attribution (CC BY) license (<http://creativecommons.org/licenses/by/4.0/>).